Modeling of kinetic, ionospheric and auroral contributions to the 557.7-nm nightglow

L. Campbell[1] and M. J. Brunger[1]

Received 9 September 2010; accepted 28 September 2010; published 19 November 2010.

[1] Emission of 557.7-nm radiation from the Earth's upper atmosphere is produced by kinetic, ionospheric and auroral excitation of oxygen atoms. The mechanisms and hence the relative contributions of these three sources are not fully understood. A ground-based mid-latitude recording of the 557.7-nm emissions over the previous solar cycle facilitates a comparison of measurements with theoretical predictions. In this paper the predicted kinetic and ionospheric contributions are simulated and compared with the observations. Semi-quantitative agreement is found between the kinetic contribution and the observations, particularly in the presence of annual, semi-annual and solar cycle variations. An observed enhancement in the emissions in the years following solar maximum is not predicted by the kinetic model. However, correlation analysis reveals a component in the observed values that is related to the auroral hemispheric power. When this extra component is included, a better fit to the pre-midnight observations over the full solar cycle is found. **Citation:** Campbell, L., and M. J. Brunger (2010), Modeling of kinetic, ionospheric and auroral contributions to the 557.7-nm nightglow, *Geophys. Res. Lett.*, *37*, L22104, doi:10.1029/2010GL045444.

1. Introduction

[2] A bright green emission line is a distinctive feature of aurora and nightglow [*Campbell*, 1895]. It was identified in 1928 as being the 557.7-nm emission due to the $O(^1S) \rightarrow O(^1D)$ transition in atomic oxygen [*Bates*, 1978]. The non-auroral sources of excitation were postulated to be collisions between oxygen atoms [*Chapman*, 1931] and recombination of O_2^+ with electrons in the ionosphere [*Nicolet*, 1954]. Rocket measurements [*Koomen et al.*, 1956] showed that the main emission was from the altitude range 80–115 km. The understanding of the kinetic source for this range was furthered by the suggestion of a two-step mechanism [*Barth*, 1961], which led to the more detailed model of *McDade et al.* [1986], while the ionospheric model has been developed further by *Sobral et al.* [1992].

[3] During solar cycle 23 *Reid and Woithe* [2007] measured the 557.7-nm emission near zenith from a ground-based mid-latitude site at Buckland Park, near Adelaide in South Australia, in years 1995–2006. While not in absolute units, the continuous record over 11 years gives the opportunity to compare with simulation results and to investigate if there is an auroral (or auroral-associated) contribution. The experimental record of *Reid and Woithe* [2007] is simulated with just the kinetic and ionospheric components, then with postulated contributions associated with auroral activity. The best correlation between calculations and observations is seen when a contribution proportional to the auroral hemispheric power is included.

2. Production Mechanisms

[4] *Barth* [1961] proposed the two-step mechanism (in which M represents O_2 or N_2):

$$\text{(R1)} \qquad O + O + M \rightarrow O_2^* + M$$

$$\text{(R2)} \qquad O_2^* + O \rightarrow O_2 + O(^1S)$$

to produce excited $O(^1S)$ atoms which subsequently radiate at 557.7 nm. *McDade et al.* [1986] produced a quantitative model that includes this mechanism and the various competing decay paths and verified it by comparison with *in situ* measurements of the densities of $O(^1S)$ atoms and the volume emission rates of 557.7-nm radiation. To implement this model the current work uses the atmospheric model NRLMSISE-00 [*Picone et al.*, 2002] and the "ap" and "f10.7" indices from http://spidr.ngdc.noaa.gov/spidr/index.jsp.

[5] In Figure 1 the current implementation of the model of *McDade et al.* [1986] is verified by emulating their calculations, using their measured values of O densities. The agreement between the calculations of McDade et al. and the emulation is not exact, most likely due to differences between the N_2 and O_2 densities in the atmospheric model used by McDade et al. and in NRLMSISE-00. The emulation is repeated using O densities calculated with NRLMSISE-00, showing that errors of ~10% can arise when using calculated O densities.

[6] The ionospheric contribution [*Nicolet*, 1954] was developed by *Sobral et al.* [1992] as:

$$\text{(R3)} \qquad O_2^+ + e \rightarrow O_2^* \rightarrow O + O + h\nu$$

where the resulting O atoms can be in the ground state $O(^3P)$ or the excited states $O(^1S)$ or $O(^1D)$. Sobral et al. determined the quantum yields of $O(^1S)$ and $O(^1D)$ in rocket flights. These are required in their expression for the 557.7-nm emission rate. In the absence of other data the current work uses these yields. Electron densities were obtained from the International Reference Ionosphere 2007 [*Bilitza and Reinisch*, 2008].

[7] $O(^1S)$ is produced in aurora by electron impact excitation of N_2 [$A^3\Sigma_u^+$] with subsequent energy transfer to $O(^1S)$, by dissociative recombination of O_2^+ and by direct electron impact excitation of O atoms [*Sharp et al.*, 1979]. As it is not possible to model these processes in detail (as measurements

[1]ARC Centre for Antimatter-Matter Studies, School of Chemical and Physical Sciences, Flinders University, Adelaide, South Australia, Australia.

0094-8276/10/2010GL045444

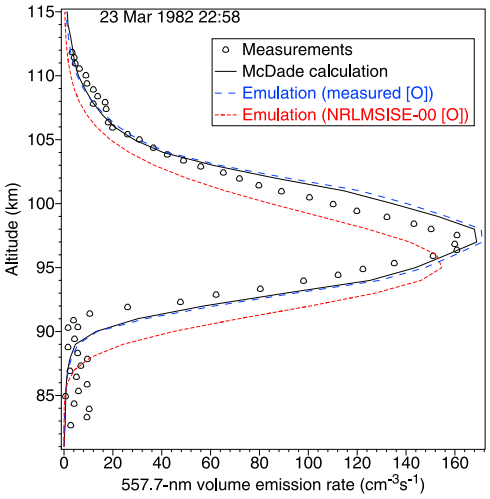

Figure 1. Measurements (○) and calculations (——) of 557.7 nm emission by *McDade et al.* [1986], and calculations in the current implementation using measured (– –) and model (- - -) O densities.

of the electron energy distribution are not available), the auroral contribution is assumed to be proportional to the hemispheric power as determined by the NOAA POES satellites [*Fuller-Rowell and Evans*, 1987].

3. Simulation of Observations

[8] To compare with measurements the 557.7-nm brightness was calculated for each day in solar cycle 23 for the 3-hour intervals 18–21, 21–0, 0–3 and 3–6 of local time at Buckland Park. This gives four time series which can be compared with the measurements and harmonic fits of *Reid and Woithe* [2007, Figure 5], which were digitized from their publication.

[9] The emissions were calculated using the theories of *Sobral et al.* [1992] and *McDade et al.* [1986] for the circumstances of the Buckland Park data. As it was found that the ionospheric component decreased rapidly after sunset, values of this were calculated at hourly intervals and only included in the 3-hour average if the solar zenith angle exceeded 108°, to exclude higher values during daylight and twilight when the photometer was not recording. The time series of the calculated components were smoothed with a 91-day running mean to allow comparison with the harmonic fits by *Reid and Woithe* [2007] as shown in Figure 2. The harmonic fits are scaled so the average intensity is equal to that for the sum of the ionospheric and kinetic components.

[10] It can be seen in Figure 2 that the 557.7-nm emission is dominated by the kinetic mechanism, with only a minor contribution from the ionospheric source. Annual and semi-annual variations are obvious in both the calculations and harmonic fits, with better quantitative agreement after midnight in both the time of the peaks and the relative heights within each year. The maximum kinetic contributions are in the years of 2000–2002, consistent with the solar maximum in April 2000 followed by an extended peak in sunspot activity through to 2002. While the kinetic contribution declines after 2002, the harmonic fits of *Reid and Woithe* [2007] indicate an enhancement in the measured emissions for 2002–2004. This suggests that an auroral component be considered, as geomagnetic activity usually has a second peak after solar maximum [*Venkatesan et al.*, 1991]. Auroral enhancements of about 400 R in 557.7-nm emissions have been observed from Adelaide, (geomagnetic latitude −45.3° [*Schaeffer and Jacka*, 1971]) but at zenith angle 80° [*Schaeffer*, 1970], rather than at zenith, so it is plausible, but not proven, that the increase in 2002–2004 could be due to auroral emissions.

4. Fitting an Auroral Component

[11] An auroral component was fitted by adding emission proportional to the hemispheric power. The fitting procedure was to postulate various values of the auroral emission at Buckland Park per gigawatt of hemispheric power and calculate the correlation coefficient between the measurements and the simulated values (ionospheric plus kinetic plus auroral) for each auroral scaling factor. (Cross correlation analysis was used rather than least-squares fitting because correlation analysis compares just the variations in shape and so is independent of any unknown constant background and the instrument sensitivity.) In Figure 3 the correlation between observations and calculations (of ionospheric plus kinetic plus auroral) is shown as a function of the postulated auroral input, for the 4 time intervals, for the years 2002–2004. For 18–21 h and 21–0 h the highest correlation is seen for an auroral contribution of about 2 rayleighs per gigawatt of hemispheric power. The contributions for the intervals after midnight are very small. This is contrary to expectations, because the auroral contribution is expected to be symmetrical around magnetic midnight, shortly before local midnight.

[12] In Figure 4 the analysis of Figure 3 is repeated for the 21–0 interval, for various time shifts in days applied to the calculated series. As the correlation coefficient is significantly larger for zero shift, it indicates that the correlation is genuine and that the digitization of the measured values was sufficiently accurate.

[13] In Figure 5 the daily calculated values for the 21–0 h interval are compared with the measurements, while 91-day running means of the calculated values are compared with the

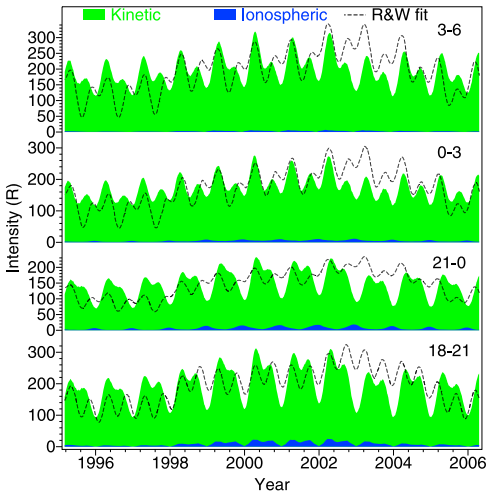

Figure 2. Calculated 557.7-nm emission for ionospheric (blue shading) and kinetic (green shading) contributions, compared with the harmonic fits (- - -) made by *Reid and Woithe* [2007] to their observations, for the 4 time intervals 18–21 h, 21–0 h, 0–3 h and 3–6 h.

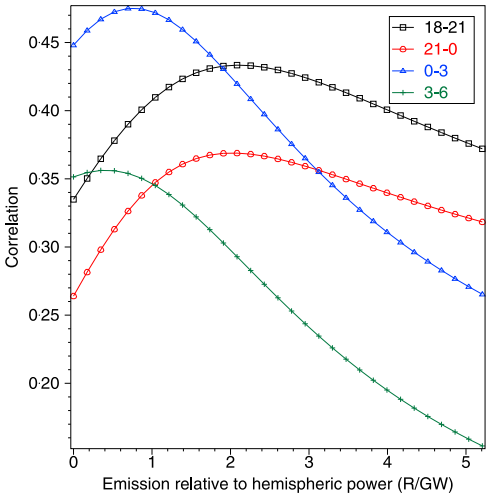

Figure 3. Correlation between observed and calculated values as a function of postulated auroral contribution for the four time intervals 18–21 h, 21–0 h, 0–3 h and 3–6 h in years 2002–2004.

harmonic fit of *Reid and Woithe* [2007]. In each case the measurements and harmonic fits are scaled to have the same average intensity as the corresponding calculated values. The auroral scaling factors (R/GW) are determined, as illustrated in Figure 3, for 3-year ranges at intervals of 3 months, accepted as genuine (or otherwise taken to be zero) if the maximum correlation at zero shift exceeds the maximum correlation calculated at all the shifts −6, −4, −2, 2, 4 and 6 days (as in the case shown in Figure 4), then smoothed with a running mean over 3 years.

[14] In Figure 5 the distribution of measured values has a greater proportion of very high values, even for the years 2002–2004 where the inferred auroral component is greatest. Hence these are not fully explained by the inclusion of the auroral component and therefore remain, as suggested by

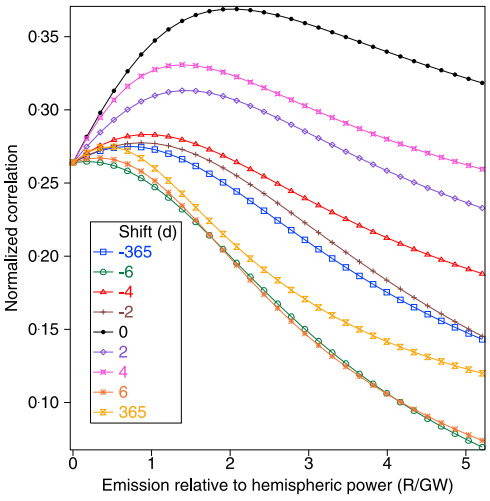

Figure 4. Correlation between observed and calculated values as a function of postulated auroral contribution for time interval 21–0 in years 2002–2004 (•). The same function is plotted for time shifts of −365, −6, −4, −2, 2, 4, 6 and 365 days applied to the simulated data, normalized to the zero-shift case at zero emission.

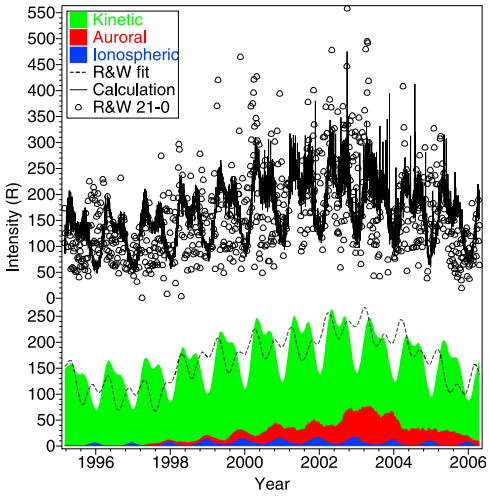

Figure 5. Daily (——) calculations of the 557.7-nm emission compared with the measurements (○) (upper part) and 91-day running means of the calculated emissions compared with the harmonic fit (- - -) of *Reid and Woithe* [2007], both for the 21–0 h interval. The ionospheric (blue shading), auroral (red shading) and kinetic (green shading) components of the 91-day running means are added vertically.

Reid and Woithe [2007], possibly due to enhancements of the O density produced by gravity waves, or tongues of enhanced airglow emissions due to planetary-scale wave disturbances.

[15] The 91-day running mean of the auroral component reaches a maximum in 2003 and the agreement between the calculated total and the harmonic fit of *Reid and Woithe* [2007] (at least in the correspondence of peak heights over the solar cycle) is better than in Figure 2. A similar result (not shown) was obtained by applying the same analysis to the 18–21 time series, but there was hardly any auroral component deduced for the data after midnight.

[16] A possible explanation is that the auroral component is mainly due to auroral-related enhancements in the electron density in the ionosphere above the levels predicted by the IRI2007 model, producing extra ionospheric emission, rather than direct electron precipitation. As seen in Figure 2, the ionospheric contribution declines through the night, so a similar decline is plausible for auroral-related enhancements. An example is that enhancements in 557.7-nm emission were detected at Adelaide in conjunction with Stable Auroral Red arcs and ascribed to reaction (R3) in the ionosphere [*Schaeffer and Jacka*, 1971].

5. Conclusions

[17] Simulations of 557.7 nm emissions from the night sky were compared with observations made over the previous solar cycle. Ionospheric and kinetic contributions were calculated using theoretical methods and empirical values from previous work. It was found that the kinetic mechanism was dominant and gave semi-quantitative agreement with the observations, showing similar annual, semi-annual and solar-cycle variations. However, the enhancement seen in the observations during the years after solar maximum was not predicted. An extra contribution, based on the auroral hemispheric power, was included and its magnitude adjusted to give the best correlation with the observations. This implied

an auroral contribution of up to 2 rayleighs per gigawatt of hemispheric power for the observations before midnight in the interval 2002-2004. Analysis of the entire solar cycle in a moving 3-year interval showed the auroral contribution was substantially larger in 2003 and accounted for the the enhancement in 557.7-nm emission seen in the observations in the years after solar maximum, but only for pre-midnight observations. The failure to identify an auroral component after midnight suggests that the auroral component may be produced by some process (such as increased electron densities) related to auroral activity, rather than direct electron precipitation.

[18] **Acknowledgments.** This work was supported by the Australian Research Council through its Centres of Excellence Program.

References

Barth, C. A. (1961), The 5577-Angstrom airglow, *Science*, *134*, 1426.

Bates, D. R. (1978), Forbidden oxygen and nitrogen lines in the nightglow, *Planet. Space Sci.*, *26*, 897–912.

Bilitza, D., and B. W. Reinisch (2008), International reference ionosphere 2007: Improvements and new parameters, *Adv. Space Res.*, *42*, 599–609.

Campbell, W. W. (1895), Note on the spectrum of the Aurora Borealis, *Astrophys. J.*, *2*, 162.

Chapman, S. (1931), Some phenomena of the upper atmoshere, *Proc. R. Soc. London A*, *132*, 353–374.

Fuller-Rowell, T. J., and D. S. Evans (1987), Height-integrated Pedersen and Hall conductivity patterns inferred from the TIROS-NOAA satellite data, *J. Geophys. Res.*, *92*, 7606–7618.

Koomen, M., R. Scolnik, and R. Tousey (1956), Distribution of the night airglow (OI) 5577A and Na *D* layers measured from a rocket, *J. Geophys. Res.*, *61*, 304–306.

McDade, I. C., D. P. Murtagh, R. G. H. Greer, P. H. G. Dickinson, G. Witt, J. Stegman, E. J. Llewellyn, L. Thomas, and D. B. Jenkins (1986), Eton 2: Quenching parameters for the proposed precursors of $O_2(b^1\ \Sigma_g^+)$ and $O(^1S)$ in the terrestrial nightglow, *Planet. Space Sci.*, *34*, 789–800.

Nicolet, M. (1954), Origin of emission of the oxygen green line in the airglow, *Phys. Rev.*, *93*, 633.

Picone, J. M., A. E. Hedin, D. P. Drob, and A. C. Aikin (2002), NRLMSISE-00 empirical model of the atmosphere: Statistical comparisons and scientific issues, *J. Geophys. Res.*, *107*(A12), 1468, doi:10.1029/2002JA009430.

Reid, I. M., and J. M. Woithe (2007), The variability of 558 nm OI nightglow intensity measured over Adelaide, Australia, *Adv. Space Res.*, *39*, 1237–1247.

Schaeffer, R. C. (1970), Airglow and auroral phenomena, Ph.D. thesis, Univ. of Adelaide, Adelaide, South Aust., Australia.

Schaeffer, R. C., and F. Jacka (1971), Stable auroral red arcs observed from Adelaide during 1967–69, *J. Atmos. Terr. Phys.*, *33*, 237–250.

Sharp, W. E., M. H. Rees, and A. I. Stewart (1979), Coordinated rocket and satellite measurements of an auroral event 2. The rocket observations and analysis, *J. Geophys. Res.*, *84*, 1977–1985.

Sobral, J. H. A., H. Takahashi, M. A. Abdu, P. Muralikrishna, Y. Sahai, and C. J. Zamlutti (1992), $O(^1S)$ and $O(^1D)$ quantum yields from rocket measurements of electron densities and 557.7 and 630.0 nm emissions in the nocturnal F-region, *Planet. Space Sci.*, *40*, 607–619.

Venkatesan, D., A. G. Ananth, H. Graumann, and Suresh Pillai (1991), Relationship between solar and geomagnetic activity, *J. Geophys. Res.*, *96*, 9811–9813.

M. J. Brunger and L. Campbell, ARC Centre for Antimatter-Matter Studies, School of Chemical and Physical Sciences, Flinders University, GPO Box 2100, Adelaide, SA 5001, Australia. (laurence.campbell@flinders.edu.au)